

Physics and Real Time Control of Tearing modes in TEXTOR

M.R. de Baar,¹ E. Westerhof,¹ W.A. Bongers,¹ I.G.J. Classen,¹ C. Domier²,
A.J.H. Donné¹, B.A. Hennen,¹ G.M.D. Hogewij¹, R.J.E. Jaspers¹, A. Lazaros,⁴
D. De Lazzari,¹ N.C. Luhmann Jr.,² P.W.J.M. Nuij,⁶ J.W. Oosterbeek,³ H.K. Park,⁵
F.C. Schüller,¹ G.W. Spakman,¹ M. Steinbuch,⁶ and the TEXTOR-Team

1. FOM-Institute for Plasma Physics Rijnhuizen, Association EURATOM-FOM, Trilateral Euregio Cluster, Nieuwegein, The Netherlands, www.rijnhuizen.nl

2. Dept. of Applied Physics, UC Davis, USA.

3. Institut für Energieforschung - Plasmaphysik, Forschungszentrum Jülich, Association EURATOM-FZJ, Trilateral Euregio Cluster, 52425 Jülich, Germany

4. National Technical University of Athens, Association Euratom-Hellenic Republic, Greece

5. Physics Department, POSTECH, Pohang, 790-784 Korea

6. Eindhoven University of Technology, Control Systems Technology Group, PO Box 513, 5600 MB Eindhoven, the Netherlands

Abstract.

The transport in and around magnetic islands has been studied by measurement of the two dimensional propagation of heat pulses generated by modulated ECRH. Inside an island with a flat temperature profile, the electron heat transport is shown to be strongly reduced with respect to the surrounding plasma. The generalized Rutherford equation is analyzed to determine the relative merits of localized heating and current drive for the stabilization of tearing modes. It is shown that for TEXTOR conditions the heating effect dominates over the effect of current drive in agreement with the experimental observations. On ITER, both are expected to be of the same order of magnitude. An optimized track-and-suppress system for tearing modes by launching angle control on TEXTOR is under development.

Introduction

High power Electron Cyclotron (EC) waves are effective in suppressing magnetic islands [1-3] and controlling sawteeth [4]. This paper reports on recent progress in the field of tearing mode (TM) physics and their suppression using high power electron cyclotron waves. TEXTOR [5] (major radius $R = 1.75$ m, minor radius $a = 0.46$ m) features a unique combination of tools that makes it very suited for this work. An Electron Cyclotron Resonance Heating (ECRH) system (140 GHz, 800 kW, 10 s) [6] is used for localized heating and current drive in the vicinity of the island. High resolution 2D Electron Cyclotron Emission Imaging (ECE-I) [7] is used for the island dynamics and transport. The Dynamic Ergodic Divertor (DED) [8] is used to reproducibly excite tearing modes by Resonant Magnetic Perturbations. A system to measure the ECE along the same sightline as the ECRH (in-Line ECE) [9] has been installed. This simplifies the real time determination of the radial location and phase of the island in support of the Real Time Control (RTC) of the ECW-beam launching.

Transport in and around magnetic islands

The cross field transport in and around magnetic islands has an important impact on the stability and evolution of (neoclassical) tearing modes. It determines the critical island size below which

the flattening of the pressure profile inside the island is incomplete. This sets the threshold for the triggering of neoclassical tearing modes [10]. The temperature perturbation induced by a local heat source can have a stabilizing effect on the tearing mode subject to the cross field transport inside the island [11]. In earlier experiments, significant stabilization of a RMP induced 2/1 tearing mode by heating inside the island was demonstrated, and a power balance analysis showed that the heat conductivity inside the island was of similar magnitude as that in the surrounding plasma [12]. In contrast, additional experiments have shown the transport inside a magnetic island to be significantly smaller than in the ambient plasma [11, 13, 14].

A number of experiments on heat pulse propagation (HPP) were done in the TEXTOR tokamak in the presence of 2/1 or 3/1 RMP induced tearing modes [15]. Here we only report on the experiments on the 2/1 mode, studied in plasmas with a toroidal field of $B_T = 2.3$ T, plasma current $I_p = 325$ kA, and central line average density $n_e = 2 \times 10^{19} \text{ m}^{-3}$. During most of the discharge, co-tangential Neutral Beam Injection (NBI) is applied at a power level of 300 kW. In these plasmas a locked 2/1 tearing mode is created by ramping the DC current in the DED-coils to 2 kA. Field line tracings have been performed of the plasma magnetic field including the vacuum field from the DED. These show that in the poloidal cross section of the ECE-I diagnostic the O-points of the 2/1 magnetic islands are close to the equatorial plane, where the ECE-I array views an area of 10 cm (radially) by 17 cm (vertically) at the low field side. Reversing the magnetic field and plasma current places the island X-point near the bottom of the ECE-I field of view. Modulated ECRH (high: 540 kW, low: 130 kW, duty cycle 50%, period 25 ms) is then applied on the high field side. The power is deposited on a minor radius well inside of the $q=2$ surface. ECE-I data from three reproducible discharges is combined to cover a radial range extending from the deposition radius inside to well outside of the 2/1 magnetic island. Figure 1 shows the results of these measurements in terms of the average temperature profile $\langle T_e \rangle$, and of the phase delay $\Delta\phi$ and amplitude ΔT_e of the temperature perturbations. The profiles are shown along a radial cross section of the ECE-I field of view either close to the island O- or close to the X-point. Near the O-point the $\langle T_e \rangle$ profile exhibits a 10 cm flat region, indicating the size and position of the magnetic island. In the same region, a strong increase in $\Delta\phi$ is observed, while ΔT_e is strongly reduced.

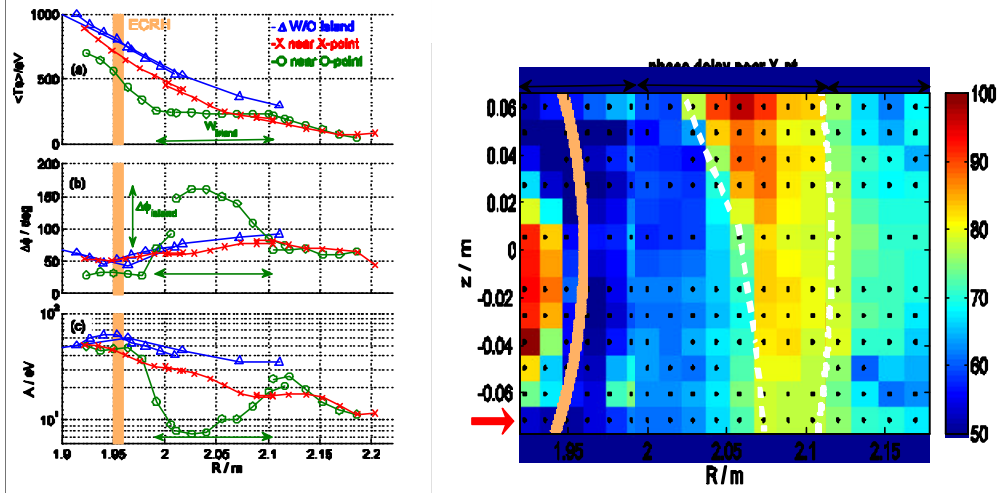


Figure 1. Left: Profiles of (from top to bottom) average temperature $\langle T_e \rangle$, phase delay $\Delta\phi$, and amplitude of the temperature perturbation. The curves show results on a cross section through the ECE-I plane near either the O- (circles) or X-point (squares) of the 2/1 magnetic island. For comparison, results from a standard 1D ECE diagnostic are given for a case without island (triangles). Right: 2D color contour plot of the phase delay near the island X-point. The solid orange curve indicates the ECRH power deposition radius. The dashed white line connects points with equal phase delay $\Delta\phi = 75^\circ$, and can be regarded as being indicative of the island separatrix. The red arrow indicates the array along which the profile on the left figure is evaluated.

These results clearly demonstrate a strong reduction of the transport of heat pulses inside the island. Near the X-point, no flattening is observed, while also a more regular, monotonic behavior both of $\Delta\phi$ as well as of ΔT_e is seen. Also shown in Fig. 1 is a 2D picture of $\Delta\phi$ near the island X-point, which illustrates that the heat flows mainly along the separatrix, through the X-point towards the plasma edge. A quantitative analysis gives a heat conductivity inside the island of $\chi_e = 0.4 \text{ m}^2/\text{s}$, whereas in the absence of a magnetic island a heat conductivity in this area of $\chi_e = 5 \pm 2 \text{ m}^2/\text{s}$.¹⁴ The latter is just slightly larger than the heat conductivity from a power balance analysis $\chi_{e,\text{PB}} = 3 \pm 1 \text{ m}^2/\text{s}$.

Relative importance of heating and current drive for tearing mode stabilization

The TEXTOR experiments on the suppression of the RMP induced tearing modes showed that the efficiency of the suppression is dominated by the effect of the island heating and is largely independent of the current driven in the island. This is consistent with the relatively low current drive efficiency under the conditions of the TEXTOR experiments. Here we provide a further theoretical comparison of the efficiencies of heating and current drive for tearing mode stabilization. The terms in the Rutherford equation describing the effect of heating, Δ'_{H} , and current drive, Δ'_{CD} , can be written in a similar way:

$$r_s \Delta'_{\text{H,CD}} = \frac{16m_0 L_q P h_{\text{H,CD}}}{p B_p w_{\text{H,CD}}^2} F_{\text{H,CD}}(w/w_{\text{H,CD}}, r_s - r_{\text{H,CD}}) \quad (1)$$

where L_q is the shear length, and B_p the poloidal field at the mode resonant surface radius r_s . A total power P is applied for heating and/or current drive. The power deposition and driven current

profile widths are indicated as w_H and w_{CD} , respectively, and can be assumed to be identical. The efficiency with which the power generates a current perturbation either through the generation of a temperature perturbation or by direct drive is indicated by h_H and h_{CD} , respectively. Finally the functions $F_{H,CD}$ account for the effects of the width of the power deposition / driven current profile relative to the island width and its localization relative to the mode resonant surface. In a tokamak the size of a typical magnetic island is generally of the same order as the width of a typical EC power deposition profile. Consequently the prime factor determining the relative importance of either heating or current drive for tearing mode stabilization is given by the respective current generation efficiencies $h_{H,CD}$, which may be written as follows

$$h_H = \frac{3 w^2}{8 \rho R n k_B c T_s} j_s \quad \text{and} \quad h_{CD} = V \frac{T_s}{n R} \quad (2)$$

where χ is the electron heat conductivity inside the island, j_s and T_s are the inductive part of the current density and temperature on the mode resonant surface, an \mathbf{z} is a normalized EC current drive efficiency depending on the wave parameters and poloidal location of the wave plasma interaction [16]. For the case of the TEXTOR experiments we obtain typically $h_H \approx 0.25$, while calculations of the EC current drive efficiency yield $h_{CD} \approx 0.001$. This confirms that heating is by far dominant. It must be noted that the wave injection in TEXTOR was not optimized towards achieving the highest possible current drive efficiency, but rather to optimize the driven current density. Note, that the ratio of the current generation efficiencies scales as $h_H : h_{CD} \sim T_s^2 / j_s$. Figure 2 compares the dimensionless quantities F_H and F_{CD} for a saturated island of width w , assuming a Gaussian power deposition profile. The calculations are static: The EC-beam is centered at the O-point, with a constant deposition width, w_{dep} . No modulation of the EC-power is applied. For small values of $w^* = w/w_{dep}$ (in ITER $w^* \sim 0.5$), F_H / F_{CD} is about 2.6. This suggests that heating can help to suppress the island below its critical value, in the regime where current drive loses its efficiency. These results and dynamic calculations of the effect will be published in [17].

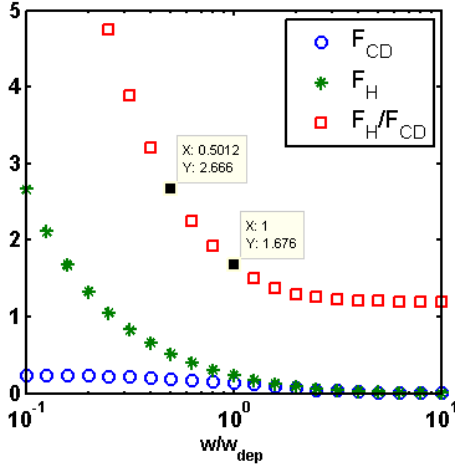


Figure 2 Comparison of the efficiency of ECCD and ECH. F_{CD} , F_H are dimensionless quantities. For $w^*=1$, F_H/F_{CD} , justifying the argument presented in [2].

Note that the heating appears more efficient than current drive. This is an important result, indicating that heating can help to suppress the island below its critical value, in the regime where current drive loses its efficiency.

Stabilization and suppression of magnetohydrodynamic (MHD) events

For reactor relevant tearing mode suppression, the high power EC-beam should be under active control [18-23] of the launching angle. An integrated installation for stabilization of MHD modes using real-time measurements in a closed control loop is being developed at TEXTOR. To this

purpose, the sensing of the modes needs to be optimized, and the gyrotron control and mechanical launcher control need to be optimized. Models need to be developed for the sensing, the actuator, and the plasma. The dynamical analysis of the electro-mechanical launcher has resulted in the design and implementation of model-based position controllers. Two algorithms capable of extracting magnetic island parameters from fluctuation measurements from electron cyclotron emission (ECE) and Mirnov diagnostics have been developed [24].

One of the problems of real-time control is the precise (radial and poloidal) localization of the island. This is required for the control the ECCD power deposition area with an accuracy of 1 to 2 cm. It is proposed to provide the feed-back signal from Electron Cyclotron Emission (ECE) measurements taken along the identical line of sight as traced by the incident ECCD mm-wave beam but in reverse direction. The advantage is that a complicated reconstruction of the plasma equilibrium is not needed and moreover geometrical optics effects like diffraction can be neglected as they will be the same for sensor signal and ECW-beam. This method implies that the ECE signal (in the order of a few nW) needs to be separated from the ECCD-beam power (in the order of 1 MW). Also, the reflection of the back reflected stray radiation (of the order of 100 W) into the radiometer has to be reduced to acceptable level.

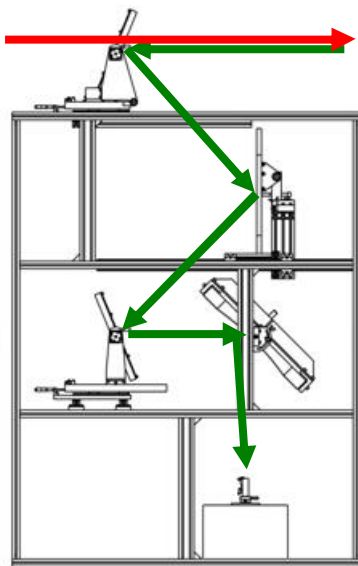


Figure 3. System for measuring ECE at frequencies close to the gyrotron frequency. The ECRH (red) is transmitted to the tokamak through an interference filter. The ECE (green) is transmitted from the tokamak and is reflected by the plate, and coupled to a radiometer via a second plate and a notch filter.

On TEXTOR this problem has been overcome by choosing the ECE signal frequency slightly different from the high power ECCD frequency and employing a sharp frequency filter to block out the high power signal from the diagnostics signal. For this purpose a Fabry-Perot (F-P) interference filter has been developed (see fig. 3). The filter is based on a quartz plate placed under an angle of 22.5° in the ECW transmission line. The plate is made resonant at the gyrotron frequency and anti-resonant at selected ECE frequencies with a periodicity of 3 GHz which determines the channel separation of the radiometer. The transmission of the ECCD-beam is optimized to 95% whilst the reflection of the backward stray radiation is minimized to 2%. The maxima in the reflected signal, determining the signal strength of the ECE signal diverted out of

the beam line, yield a 37% reflection coefficient. At the resonant frequency the power absorption of the plate is 5%. The diagnostic ECE signal is subsequently passed through a second quartz plate placed under 22.5° in order to further reduce stray gyrotron radiation. A focusing mirror shapes the microwave beam into the antenna pattern of the corrugated receiving horn of the radiometer. Before entering the radiometer, a -80 dB, 140 GHz notch filter with a bandwidth of 100 MHz serves as a third attenuation step of stray gyrotron radiation. In addition, a pin-switch protects the radiometer from spurious modes produced by the gyrotron during switch-on and switch-off at frequencies that differ slightly from the 140 GHz and are therefore not blocked by the notch filter. The ECE spectrum is monitored in a frequency band of 132 to 148 GHz, which under normal TEXTOR operating conditions covers about 1/3 of the plasma cross-section on the high field side. The first measurements obtained with the novel in-line ECE diagnostics during ECRH clearly demonstrate the potential of identifying various structures in the ECE spectrum, like sawtooth inversion and rotating magnetic islands [9]. These measurements motivate the further development and the implementation of a similar ECCD aligned ECE system for NTM control in larger fusion machines. For this purpose a new scheme has been designed for implementation on ASDEX-Upgrade (AUG). A possible implementation of such a system on AUG, based on waveguides equipped with a fast directional switch FADIS, is presented in [25]. A possible further development for ITER is also discussed.

Summary and Conclusions

TEXTOR combines a number of features that make it well suited for the research in tearing modes and their stabilization. The transport inside magnetic islands has been probed extensively by heat pulse propagation techniques. The results have shown the heat conductivity in the flattened part of the temperature profile inside the island to be strongly reduced in comparison with heat conductivity in the ambient plasma. This may have consequences for the determination of the critical island size for the destabilization of neoclassical tearing modes. A theoretical analysis of the relative merits of pure heating and direct current drive explains the observation that in the TEXTOR experiments the mode suppression is dominated by the effect of heating inside the island. ITER relevant static calculations show that for small values of w^* heating appears about 2.6 times more efficient than current drive [17]. This is an important result, indicating that heating can help to suppress the island below its critical value, in the regime where current drive loses its efficiency.

A system for closed loop real time track-and-suppress of tearing modes is under development. The detection branch uses the same line of sight as the gyrotron, which simplifies the interpretation of the radial location of the mode and its phase considerably. This detection branch has been tested successfully.

Acknowledgement

This work, supported by the European Communities under the contract of Association between EURATOM/FOM, was carried out within the framework of the European Fusion Programme and EFDA. The views and opinions expressed herein do not necessarily reflect those of the European Commission. This work was supported by NWO-RFBR grant nr. 047.016.016.

References

- [1] A. Isayama et al., *Plasma Phys. Control. Fusion* 42 (2000) L37.
- [2] G. Gantenbein et al., *Phys. Rev. Lett.* 85(6) (2000) 1242.
- [3] C.C. Petty et al., *Nucl. Fusion* 44 (2004) 243.
- [4] A. Mück et al., *Plasma Phys. Control. Fusion* 47 (2005) 1633.
- [5] U. Samm., *Fusion Sci. Techn.* 47 (2005) 73.
- [6] E. Westerhof, et al., *Fusion Sci. Techn.* 47 (2005) 108.
- [7] C.W. Domier, et al., *Rev. Sci. Instrum.* 77 (2006) 10E924.
- [8] K.H. Finken (ed), *Fusion Eng. Des.* (special issue DED) 37 (1997) 335.
- [9] J.W. Oosterbeek, *Rev. Sci. Inst.* **79**, 093503 (2008)
- [10] R. Fitzpatrick, *Phys. Plasmas* 2 (1995) 825.
- [11] P.C. de Vries, et al., *Plasma Phys. Control. Fusion* 39 (1997) 439.
- [12] I.G.J. Classen, et al., *Phys. Rev. Lett.* 98 (2007) 035001.
- [13] F. Salzedas, et al., *Phys. Rev. Lett.* 88 (2002) 075002.
- [14] S. Inagaki, et al., *Phys. Rev. Lett.* 92 (2004) 055002.
- [15] G.W. Spakman et al., *Nucl. Fusion* **48** (2008)
- [16] R. Prater, *Phys. Plasmas* 11 (2004) 2349.
- [17] D. de Lazzari et al., to be submitted to *Nucl. Fusion*.
- [18] R.J. La Haye et al., *Phys. Plasmas* 13 (2006).
- [19] D.A. Humphreys et al., *Phys. Plasmas* 13 (2006).
- [20] S. Alberti et al., *Nucl. Fusion* 45 (2005) 1224.
- [21] A. Manini et al., *Fusion Eng. Des.* 82 (2007) 995.
- [22] W. Treutterer et al., *Fusion Eng. Des.* 83 (2008) 300.
- [23] J. Berrino et al., *IEEE Trans. Nucl. Sci.* 53(3) (2006) 1009.
- [24] B. A. Hennen, *Proc. 25th SOFT conference, FS&T* (2008)
- [25] W.A. Bongers et al., Accepted for publication *Proc. 15th Conf. on EC waves*, (2008)